Advanced Engine Cooling System Subjected to Ram Air Effect—Nonlinear Adaptive Multiple Input and Multiple Output (NAMIMO) Control

Tianwei (Thomas) Wang and John Wagner, *Senior Member, IEEE*

***Abstract*—Advanced engine cooling systems typically replace the traditional mechanical cooling actuators with electrical controlled ones to reduce unnecessary power losses. The real time adjustment of the pump, valve, and radiator fans allow the engine temperature to be more accurately regulated. This paper investigates a nonlinear adaptive multi-input and multi-output (NAMIMO) controller to operate the valve and radiator fans to control the engine temperature under different operating conditions. A nonlinear adaptive backstepping (NAB) control strategy and a state flow (SF) control law are introduced for comparison. An experimental laboratory station has been fabricated to evaluate the proposed controllers. The test results show that the NAMIMO controller can regulate the engine temperature to a desired value ($|e| < 0.5\,^{\circ}$C at steady state) and compensate for unknown heat loads and ram air effects. In contrast, the NAB control law consumes the least radiator fan power but realized a larger average temperature tracking error (40% greater than NAMIMO controller) and longer response time (34% greater than NAMIMO controller) and shows weakness when the heat load is low. Finally, the SF controller, characterized by greater oscillation and electrical power consumption (18.9% greater than the NAMIMO controller), was easy to realize and maintained the engine temperature within $|e| < 0.5\,^{\circ}$C. The main technical contribution of the study is a nonlinear control strategy which regulates the engine temperature while compensating for unknown heat loads and ram air effects.**

***Index Terms*—Automotive cooling, experimental test, mathematical model, nonlinear adaptive multi-input and multi-output (NAMIMO) control, ram air effect.**

I. Introduction

MANY countries have issued fuel economy and/or carbon dioxide emission standards to improve the efficiency of internal combustion engines and reduce their tailpipe greenhouse gases. By the year 2021, the target fuel economies are 46.8 miles per gallon (MPG) and 56.9 MPG for light passenger cars in the United States and European Union, respectively [1], [2]. According to the United States Environment Protective Agency (EPA) [3], oil savings from the current vehicle fleet is due to updated gasoline engine technologies. However, the contribution from engine cooling system innovation has not yet been widely implemented. According to Heywood [4], approximately 25% of the total energy generated from the combustion process is lost to the cooling system (25% is the effective power, 40% to exhaust gas, and 5% lost in friction). Predictably, applying updated technology on the engine cooling system has great potential to promote improved fuel economy. Page *et al.* [5] proposed that the fuel economy gains for a vehicle equipped with a smart cooling system are expected to be as high as 15.6%.

Typically, the current engine cooling system is designed to keep the engine temperature in an acceptable range even during the worst working conditions [6]. In a traditional setup, the mechanical pump and radiator fan(s) are indirectly connected with the crankshaft. A wax-based thermostat is mounted to regulate the coolant flow route through the radiator. Although the system reliability has been repeatedly demonstrated in past decades, two limitations exist. On the one hand, the mechanical coupling leads the operation of the actuators (pump and radiator fans) to be dependent on the engine speed which cannot be controlled accurately for cooling purposes and typically yields engine overcooling. It has been suggested that overcooling can degrade the engine performance [7], increase the lubricate oil friction [8] and necessitate more work than needed by this subsystem which lead a lower fuel economy. On the other hand, the mechanical connections, such as accessory belts and clutches, generate unnecessary energy losses but provide proven interface.

An advanced engine cooling system introduces the concept of "thermal management" by regulating the engine coolant to a precise working temperature with minimum power consumption [9]. A smart engine cooling system updates the mechanical pump and radiator fan(s) with electrical controlled components and replaces the wax-based valve with a 3-way computer controlled smart valve. With these features, each actuator can be operated accurately to achieve a certain heat rejection requirement with minimum energy utilization theoretically. Besides, assorted sensors are mounted to monitor the system's dynamics and operating environment. The electronic control unit (ECU) hosts the control strategy and sends out commanded signals to the actuators based on the real time system dynamics and prescribed control algorithm. The diagram of an advanced cooling system is shown in Fig. 1.

Manuscript received January 6, 2016; revised June 4, 2016 and September 12, 2016; accepted February 22, 2017. Date of publication March 2, 2017; date of current version September 15, 2017. The review of this paper was coordinated by Prof. J. Wang.

The authors are with Clemson University, Clemson, SC 29634 USA (e-mail: tianwew@g.clemson.edu; jwagner@clemson.edu).

Color versions of one or more of the figures in this paper are available online at http://ieeexplore.ieee.org.

Digital Object Identifier 10.1109/TVT.2017.2676987

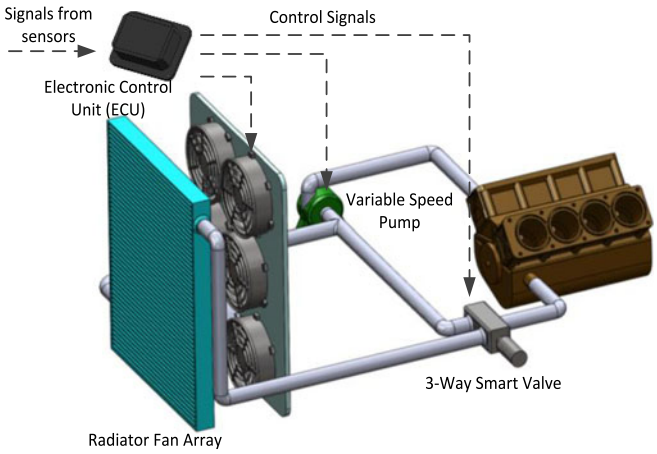

Fig. 1. Advanced internal combustion engine cooling system.

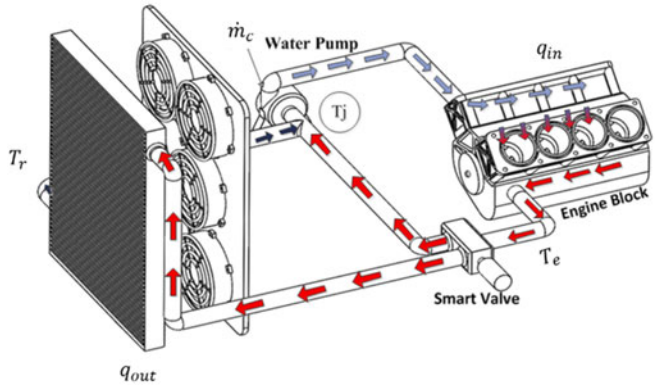

Fig. 2. Engine cooling system and coolant flow directions.

To complement the updated configuration of the cooling system, assorted control strategies have been proposed for these actuators. Wang *et al.* [10] explored an optimal fan matrix control strategy to minimize the radiator fan power while achieving the requested heat rejection. Wang and Wagner [11] proposed a Lyapunov based backstepping nonlinear control strategy to adjust the radiator fan matrix operation to track a desired engine temperature while compensating the unknown heat input with minimum power consumption. Salah *et al.* [12], [13] designed nonlinear control strategies to control the smart valve position or the coolant pump speed to realize the desired engine temperature. Wagner *et al.* [7] investigated the electrical water pump and a thermostat valve control approach to achieve faster engine warm-up. Tao and Wagner [14] developed a model predictive controller to regulate the compressor speed in vapor compression systems to track the cooling air temperature and stabilize the hybrid electric vehicle battery core temperatures. Butt *et al.* [15], [16] investigated input-output linearization and model-predictive control strategies by implementing the experimental test on a small prototype configuration. Khodabakhshian *et al.* [17] proposed a model predictive control method and a global optimal solution to improve the fuel efficiency of conventional trucks.

This paper investigates a nonlinear adaptive MIMO (NAMIMO) controller for the operation of the cooling system actuators. The remainder of the paper is organized as follows. A detailed mathematical model and system analysis will be presented in Section II. The NAMIMO controller with stability analysis will be introduced in Section III. Section IV contains the fully experimental test bench description, followed by the discussion of test results in Section V. Finally, the conclusion will be offered in Section VI. Two other controller designs are offered in the Appendices.

II. Mathematical Models

To investigate the smart automotive engine cooling system, a lumped parameter mathematical model has been formulated to describe the thermal dynamics. The cooling system configuration with fluid flow direction is displayed in Fig. 2. The color variation indicates the coolant temperature changes. In this research, three assumptions have been imposed on the thermal system:

A1: No heat losses occur in the system other than forced convection through the radiator.

A2: Engine heat load due to the combustion process can be removed by the cooling system once warm up has been accomplished.

A3: The desired engine and radiator working temperatures are assumed to be quasi constants.

Te Tr为常数

A. Cooling System Thermal Dynamics

Two heat exchangers, engine and radiator, can be considered in a standard automotive cooling system. The governing equations for these two thermal components can be described as

$$C_e\dot{T}_e = -\dot{m}_c Cp_c\left(T_e - T_j\right) + q_{\text{in}} \tag{1}$$

$$C_r\dot{T}_r = \dot{m}_c HCp_c\left(T_e - T_r\right) - q_f - q_{\text{ram}} \tag{2}$$

where the variables T_e and T_r denote the engine and radiator temperatures. The variable $\dot{m}_c$ represents the coolant mass flow rate. The parameters Cp_c, C_e, and C_r are the heat capacity of the coolant, engine, and radiator at constant pressure. The term q_{in} is the heat load generated by the combustion process. The variable H represents the smart valve position with $H = 0$ and $H = 1$ corresponding to fully closed and open positions, respectively.

The coolant temperature at the junction T_j depends on the mixing temperature of the fluids flowing through the bypass and radiator, or

$$T_j = (1 - H)\,T_e + HT_r \tag{3}$$

The variables q_f and q_{ram} in equation (2) describe the heat rejected due to the radiator fan(s) and the ram air effect. The explicit expression for q_f can be written as

$$q_f = \dot{m}_f Cp_a\left(T_r - T_\infty\right) \tag{4}$$

where Cp_a is the heat capacity of the air, and the variable T_∞ is the ambient temperature. According to a previous study [10], the air mass flow rate due to the radiator fans $\dot{m}_f$ is a nonlinear function of the number of fans n and the radiator fan speed

N_{fan} so that $\dot{m}_f = F(N_{\text{fan}}, n)$. The ram air effect q_{ram} can be expressed as

$$q_{\text{ram}} = f\left(v_{\text{speed}}, v_{\text{wind}}, \alpha_{\text{wind}}, T_r, T_\infty\right) \tag{5}$$

where v_{speed} and v_{wind} are the vehicle and wind speeds. The term α_{wind} denotes the attack angle of the wind with respect to the vehicle's radiator position.

B. Dynamic Analysis of Open Loop System

The open loop behavior of the cooling system's thermal dynamics can be analyzed to determine the operating space. This effort offer insight into the control system design to accommodate the desired engine heat rejection. First, substitute equation (3) into (1) so that the engine temperature becomes

$$C_e \dot{T}_e = -\dot{m}_c H C p_c \left(T_e - T_r\right) + q_{\text{in}}. \tag{6}$$

Now, add (2) and (6) together such that the rate of the entire cooling system heat change may be expressed as

$$C_e \dot{T}_e + C_r \dot{T}_r = q_{\text{in}} - q_f - q_{\text{ram}}. \tag{7}$$

Equation (7) indicates that the system heat, $C_e T_e + C_r T_r$, depends on the difference between the engine heat load, q_{in}, and the active, q_f, and ram air, q_{ram}, heat rejected through the radiator. Equation (4) may be substituted into equation (2), and then rewrite equations (2) and (6) rewritten in a compact state space form as

$$\dot{x}_O = A_O x_O + b_O \tag{8}$$

where

$$x_O = \begin{bmatrix} T_e & T_r \end{bmatrix}^T \tag{9a}$$

$$A_O = \begin{bmatrix} \dfrac{-\dot{m}_c H C p_c}{C_e} & \dfrac{\dot{m}_c H C p_c}{C_e} \\ \dfrac{\dot{m}_c H C p_c}{C_r} & \dfrac{-\dot{m}_c H C p_c - \dot{m}_f C p_a}{C_r} \end{bmatrix} \tag{9b}$$

$$b_O = \begin{bmatrix} \dfrac{q_{\text{in}}}{C_e} \\ \dfrac{\dot{m}_f C p_f T_\infty - q_{\text{ram}}}{C_r} \end{bmatrix}. \tag{9c}$$

Note that A_O is not a constant matrix but a function of the control input. The equilibrium point of this system (constant solution to (8)) T_e^* and T_r^* can be calculated as

$$\dot{x}_O = 0; \quad \begin{bmatrix} T_e^* \\ T_r^* \end{bmatrix} = \begin{bmatrix} \dfrac{q_{\text{in}}}{\dot{m}_c H C p_c} + \dfrac{q_{\text{in}} - q_{\text{ram}}}{\dot{m}_f C p_a} + T_\infty \\ \dfrac{q_{\text{in}} - q_{\text{ram}}}{\dot{m}_f C p_a} + T_\infty \end{bmatrix}. \tag{10}$$

Equation (10) implies that the fixed point exists only when $\dot{m}_c H C p_c$ and $\dot{m}_f C p_a$ are non-zero (i.e., the pump and radiator fans are not idle and the valve is not in a fully closed position). The sign of eigenvalues of the open-loop system state matrix A_O, $\lambda_{Ao1,2}$ can be determined by the matrix invariant

$$\lambda_{Ao1} + \lambda_{Ao2} = tr\left(A_O\right) = \frac{-\dot{m}_{\text{cool}} H C p_{\text{cool}}}{C_e} + \frac{-\dot{m}_{\text{cool}} H C p_{\text{cool}} - \dot{m}_f C p_a}{C_r} < 0 \tag{11a}$$

$$\lambda_{Ao1}\lambda_{Ao2} = det\left(A_O\right) = \frac{\dot{m}_c H C p_{\text{cool}} \dot{m}_f C p_a}{C_e C_r} > 0. \tag{11b}$$

Equations (11a) and (11b) reveals that the eigenvalues for the matrix A_O are always negative. As a result, the engine and radiator temperatures (T_e, T_r) can approach the equilibrium point (T_e^*, T_r^*) as time goes to infinity.

On the other hand, the equilibrium point may not exist for two special situations.

Case 1: Coolant pump is shut off or the smart valve is at a fully closed position, (i.e., $\dot{m}_c H = 0$). In this situation, (8) becomes

$$\begin{bmatrix} \dot{T}_e \\ \dot{T}_r \end{bmatrix} = \begin{bmatrix} 0 & 0 \\ 0 & \dfrac{-\dot{m}_f C p_a}{C_r} \end{bmatrix} \begin{bmatrix} T_e \\ T_r \end{bmatrix} + \begin{bmatrix} \dfrac{q_{\text{in}}}{C_e} \\ \dfrac{\dot{m}_f C p_f T_\infty - q_{\text{ram}}}{C_r} \end{bmatrix} \tag{12}$$

which demonstrates that the engine temperature, T_e, keeps increasing since $\dot{T}_e$ is always positive when $q_{\text{in}} > 0$. This situation may happen during an engine warm up (i.e., cold start) scenario.

Case 2: Radiator fans are shut off, $q_f = 0$, such that equation (8) becomes

$$\begin{bmatrix} \dot{T}_e \\ \dot{T}_r \end{bmatrix} = \begin{bmatrix} \dfrac{-\dot{m}_c H C p_c}{C_e} & \dfrac{\dot{m}_c H C p_c}{C_e} \\ \dfrac{\dot{m}_c H C p_c}{C_r} & \dfrac{-\dot{m}_c H C p_c}{C_r} \end{bmatrix} \begin{bmatrix} T_e \\ T_r \end{bmatrix} + \begin{bmatrix} \dfrac{q_{\text{in}}}{C_e} \\ \dfrac{-q_{\text{ram}}}{C_r} \end{bmatrix}. \tag{13}$$

Consider equation (7) first. If $q_f = 0$ and the ram air effect, q_{ram}, is greater than the heat load, q_{in}, then the entire system heat will decrease. Predictably, a pump-valve combination control strategy exists to maintain the engine temperature, T_e, at the desired point. This phenomenon may be considered as highway operation with abundant ram air. On the other hand, if $q_f = 0$, and the ram air effect q_{ram}, is less than the heat load, q_{in}, then the system heat will increase. According to the cooling system configuration, it is not possible to maintain the engine temperature T_e for the heat input directly supplied to the engine. This corresponds to a vehicle under high load and low speed (not enough ram air) which requires the radiator fans to be operated to prevent overheating.

III. Control Strategies

A nonlinear adaptive multi-input and multi-output (NAMIMO) controller has been developed to regulate the engine and radiator temperatures, T_e and T_r. The challenge of this controller design is from two uncertain system variables. Namely, the heat load generated by the combustion process, q_{in}, and the heat rejection due to the ram air effect, q_{ram}. As these two entities cannot be easily measured, the controller must compensate for them. For comparison purposes, two other control methods

have been considered, a nonlinear adaptive backstepping (NAB) and a state flow (SF). The reader is referred to Appendixes A and B for more details of the NAB and SF controllers.

带有observer的tracking

A. Closed-Loop Feedback System Description

To evaluate the temperature tracking control objective, the tracking error signals e and r are defined as

$$e = T_{ed} - T_e \tag{14}$$

$$r = T_{rd} - T_r \tag{15}$$

where T_{ed} and T_{rd} represent the desired engine and radiator temperatures, respectively. Note that the set point temperatures are assumed constant (*A3*) so that $\dot{T}_{ed} = \dot{T}_{rd} = 0$. See to Section III-C for further discussion of the desired reference values T_{ed} and T_{rd}.

The control objective is to ensure that the engine and radiator temperatures track the desired values, such that

$$e, r \to 0 \quad \text{as} \quad t \to \infty \tag{16}$$

Furthermore, the controller must compensate for the unknown system parameters q_{in} and q_{ram} or

$$\tilde{q}_{\text{in}} = q_{\text{in}} - \hat{q}_{\text{in}} \to 0, \tilde{q}_{\text{ram}} = q_{\text{ram}} - \hat{q}_{\text{ram}} \to 0 \text{ as } t \to \infty \tag{17}$$

where $\hat{q}_{\text{in}}$ and $\hat{q}_{\text{ram}}$ are the estimated variables of the heat load and ram air effect, respectively.

Now, substitute equations (4), (14), and (15) into equations (2) and (6), so that the closed-loop feedback system can be formulated as

$$\dot{e} = \frac{u_1 C p_c}{C_e}\left(T_{ed} - e - T_{rd} + r\right) - \frac{q_{\text{in}}}{C_e} \tag{18}$$

$$\dot{r} = -\frac{u_1 C p_c}{C_r}\left(T_{ed} - e - T_{rd} + r\right) + \frac{u_2 C p_a \left(T_{rd} - r - T_\infty\right) + q_{\text{ram}}}{C_r} \tag{19}$$

where $u_1 = \dot{m}_c H = G(H, N_{\text{pump}})$ denotes the system input '1' which is an inseparable system input of the 'pump-valve combination.' The second system input, '2', or $u_2 = \dot{m}_f = F(N_{\text{fan}}, n)$ corresponds to the operation of the radiator fans.

B. NAMIMO Controller Design and Stability Analysis

The feedback system inputs, u_1 and u_2, and the estimated parameters $\hat{q}_{\text{in}}$ and $\hat{q}_{\text{ram}}$ can be designed based on the definitions above as

$$u_1 = \dot{m}_c H = \frac{\hat{q}_{\text{in}} - C_e k_1 e}{C p_c \left(T_e - T_r\right)} \tag{20}$$

$$u_2 = \dot{m}_f = \frac{u_1 C p_c \left(T_e - T_r\right) - \hat{q}_{\text{ram}} - C_r k_2 r}{C p_a \left(T_r - T_\infty\right)} \tag{21}$$

???

$$\hat{q}_{\text{in}} = -\frac{1}{C_e}\int_{t_0}^{t} e d\tau \tag{22}$$

$$\hat{q}_{\text{ram}} = \frac{1}{C_r}\int_{t_0}^{t} r d\tau \tag{23}$$

where $k_{1,2}$ are the positive controller gains.

To demonstrate the stability of the feedback system, substitute (20) and (21) into (18) and (19), and take the derivative of equations (22) and (23) over time and substitute (17), which leads to

$$\dot{e} = -k_1 e - \frac{\tilde{q}_{\text{in}}}{C_e} \tag{24}$$

$$\dot{r} = -k_2 r + \frac{\tilde{q}_{\text{ram}}}{C_r} \tag{25}$$

$$\dot{\tilde{q}}_{\text{in}} = \dot{q}_{\text{in}} + \frac{1}{C_e} e \tag{26}$$

$$\dot{\tilde{q}}_{\text{ram}} = \dot{q}_{\text{ram}} - \frac{1}{C_r} r. \tag{27}$$

In this paper, the slow varying heat transfers in and out of the system is considered, i.e., $\dot{q}_{\text{in}} = \dot{q}_{\text{ram}} = 0$. Next, rewrite (24)–(27) in compact form as

$$\dot{x}_c = A_c x_c + b_c \tag{28}$$

where

$$x_c = \begin{bmatrix} e & r & \tilde{q}_{\text{in}} & \tilde{q}_{\text{ram}} \end{bmatrix}^T \tag{29a}$$

$$A_c = \begin{bmatrix} -k_1 & 0 & -1/C_e & 0 \\ 0 & -k_2 & 0 & 1/C_r \\ 1/C_e & 0 & 0 & 0 \\ 0 & -1/C_r & 0 & 0 \end{bmatrix} \tag{29b}$$

$$b_c = \begin{bmatrix} 0 & 0 & 0 & 0 \end{bmatrix}^T. \tag{29c}$$

The equilibrium point for equation (28) becomes

$$\dot{x}_c = 0; \quad \begin{bmatrix} e^* \\ r^* \\ \tilde{q}^*_{\text{in}} \\ \tilde{q}^*_{\text{ram}} \end{bmatrix} = [0]. \tag{30}$$

The eigenvalues of the closed loop state matrix A_c may be written as

$$\begin{bmatrix} \lambda_{A_c 1,2} \\ \lambda_{A_c 3,4} \end{bmatrix} = \begin{bmatrix} -\frac{k_1}{2} \pm \sqrt{\frac{k_1^2}{4} - \frac{1}{C_e^2}} \\ -\frac{k_2}{2} \pm \sqrt{\frac{k_2^2}{4} - \frac{1}{C_r^2}} \end{bmatrix}. \tag{31}$$

Equation (31) indicates that the eigenvalues always have negative real parts with the designed controller, equations (20)–(23) applied (both gains must be positive). It demonstrates an attractor at the equilibrium point [0]. Note that, the eigenvalues may or may not have an imaginary part dependent on the selected controller gains $k_{1,2}$, which indicates that the system may or may not oscillate.

Remark 1: Internal combustion engines generate a certain amount of heat based on the size and configuration. As a result, the estimated parameter $\hat{q}_{\text{in}}$ has the upper bound $\hat{q}_{\text{in}} \le q_{inu}$.

Remark 2: Vehicle movement and wind speed can remove a finite amount of heat so that the estimated parameter $\hat{q}_{\text{ram}}$ has the upper bound $\hat{q}_{\text{ram}} \le q_{ramu}$.

C. Selection of Desired Reference Values

The desired engine temperature T_{ed} may be selected according to the vehicle's operation to realize the imposed working condition. On the other hand, the selection of the desired radiator temperature T_{rd} should be based on the power consumption. It is important to carefully determine the system reference values since they impact the controller's performance and the actuator power usage.

Remark 3: Radiator fans consume the most electric power (about 85%) followed by the coolant pump (about 15%) and the smart valve (less than 1%) for a standard electro-mechanical thermal management system. One of the best control strategies is to decrease the radiator fan "on time" to reduce the power demand [18], [19].

Consider the steady state scenario for the feedback system in equation (18), when $e = \dot{e} = r = 0$. This operating condition allows the closed-loop feedback system to be rewritten at the equilibrium point as

$$0 = \frac{u_1 Cp_c}{C_e}\left(T_{ed} - T_{rd}\right) - \frac{q_{\text{in}}}{C_e} \tag{32}$$

which leads to

$$T_{ed} - T_{rd} = \frac{q_{\text{in}}}{u_1 Cp_c}. \tag{33}$$

Equation (33) implies that the temperature difference between the two system references $T_{ed} - T_{rd}$ is a function of the heat load q_{in} and the pump–valve combination u_1. Consider the working spectrum of the pump-valve combination $u_{1\min} \le u_1 < u_{1\max}$. The range of possible temperature differences in equation (33) can be expressed as

$$\frac{q_{\text{in}}}{u_{1\max} Cp_c} < T_{ed} - T_{rd} \le \frac{q_{\text{in}}}{u_{1\min} Cp_c} \tag{34}$$

where $u_{1\min} = \dot{m}_{c\min} H_{\min}$ and $u_{1\max} = \dot{m}_{c\max} H_{\max}$. In addition, the radiator temperature cannot generally be controlled lower than the ambient temperature T_∞. As a result, T_{rd} may be bounded between

$$T_{ed} - \frac{q_{\text{in}}}{u_{1\max} Cp_c} > T_{rd} \ge MAX\left(T_\infty, T_{ed} - \frac{q_{\text{in}}}{u_{1\min} Cp_c}\right). \tag{35}$$

From a power consumption perspective (see Remark 3), the coolant pump and smart valve should be operated at maximum capacity ($u_1 = u_{1\max}$) to allow a possible decrease in the radiator fan speed. Specifically, the target radiator temperature expression becomes $T_{rd} = T_{ed} - \frac{q_{\text{in}}}{u_{1\max} Cp_c}$.

In practice, the heat load, q_{in}, cannot generally be measured in real time. For the NAMIMO controller, T_{rd} can be considered to be a function of the estimated heat load, $\hat{q}_{\text{in}}$. However, the estimated heat load, $\hat{q}_{\text{in}}$, is an integral term of the time-variant engine temperature tracking error e as shown in (22). Further, the operation of the radiator fan is characterized by a large time constant to regulate the radiator temperature [18]. A time-varying desired radiator temperature, T_{rd}, will cause a large fluctuation of the radiator fan speed which is not applicable. To compensate for the fluctuation, a "slow change" reference should be prescribed. In this project, based on the baseline calibrations,

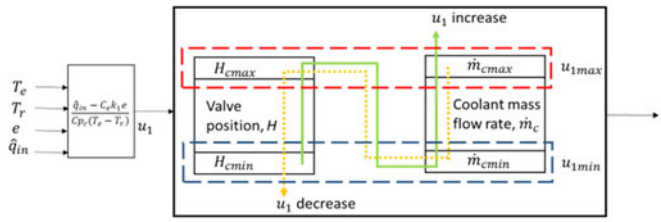

Fig. 3. Calibration turning method for the system input '1', u_1, increasing (solid green line) and deceasing (dotted orange line) with thermal loading.

the selection of T_{rd} shall be defined as a step function with

$$T_{rd} = \begin{cases} T_{rdl}; & \hat{q}_{\text{in}} \ge \hat{q}_{inh} \\ T_{rdm}; & \hat{q}_{inh} > \hat{q}_{\text{in}} > \hat{q}_{inl} \\ T_{rdh}; & \hat{q}_{\text{in}} \le \hat{q}_{inl} \end{cases} \tag{36}$$

where T_{rdh}, T_{rdl}, and T_{rdm} are the selected radiator temperatures. Similarly, $\hat{q}_{inh}$ and $\hat{q}_{inl}$ are the heat input thresholds according to the baseline calibration.

D. Calibration Approach for System Input u_1 and u_2

From a power consumption viewpoint (see Remark 3), the coolant pump consumes much more power than the valve. Equation (20) offers the system input '1', pump-valve combination, u_1. An engineering calibration approach can be formulated. For example, in Fig. 3, as the value of the pump-valve combination u_1 increases, first calibrate the valve position from $H_{\min}$ to $H_{\max}$ while keeping the coolant mass flow rate at its lower limitation, $\dot{m}_c = \dot{m}_{c\min}$. As u_1 increases, the pump speed can then be raised once the valve position has reached its maximum value (green solid line). On the other hand, when the system input '1' u_1 decreases, the coolant mass flow rate is first adjusted followed by the valve closing (dotted orange line).

A previous study proposed an optimal radiator fan operating strategy (i.e., system controller u_2), for various heat loads [10]. In this research, the number of fans is selected as $n = 6$ to simplify the testing and analysis. In other words, the same operating path is traced for all thermal load variations.

IV. Experimental Test Bench

An experimental laboratory bench was created to evaluate the performance of the proposed control strategies. A static 6.8 L International Truck V8 diesel engine was selected as the test subject. Low pressure (LP) steam was supplied to emulate the heat generated by the engine's combustion process using a shell-tube heat exchanger with the engine coolant and the steam. The heat supplied to the system can be estimated using the coolant dynamics given as

$$q_{\text{in}} = \dot{m}_c Cp_c \left(T_{HI} - T_{HO}\right) \tag{37}$$

where T_{HI} and T_{HO} are the heat exchanger inlet and outlet temperatures, respectively.

To redirect the coolant flow path, a worm gear assembly driven three way smart coolant valve was installed. An AC motor driven pump was mounted to circulate the coolant. Six CAN

Fig. 4. Picture of experimental test bench. (a) Valve, (b) coolant pump, (c) wind tunnel radiator fans, and (d) ram air axial fan.

(Controlled Area Network) bus controlled 24V brushless DC fans were installed in a wind tunnel along with a radiator. Four Omega J-type thermocouples measured the temperature at the heat exchanger's inlet T_{HI} and outlet T_{HO} and the engine's and radiator's outlets T_e and T_r. The coolant flow rate was measured using a turbine type flow meter. The valve's position was monitored by a potentiometer. The working state of the radiator fans was obtained through the CAN bus signals. An auxiliary axial fan, Triangle SPL4223, was located in front of the fan matrix to simulate the ram air effect $q_{\rm ram}$. The test bench is shown in Fig. 4 and a complete experimental bench description can be found in [11].

V. Presentation and Discussion of Test Results

A series of experimental tests were conducted to evaluate the performance of the three proposed control laws. The design of experiment and the parameters values used in the tests are listed in Table I and II. For each test, a step heat input was applied at time $t = [1\ \text{min}\,(60\ \text{s}),\ 11\ \text{min}\,(660\ \text{s}),\ 21\ \text{min}\,(1260\ \text{s})]$. The ram air axial fan was turned 'ON' in Tests 2, 4, and 6 for time $t \geq 1$ min *(60 s)*. In Tests 1-6, due to the limitation of the experimental test bench, the pump speed cannot be adjusted automatically, so the coolant flow rate is fixed at $\dot{m}_c = \dot{m}_{c\max} = 1$ kg/s. The valve was operated in real time, so the system input '1' corresponded to $u_1 = \dot{m}_{c\max} H$. The radiator fans were operated between 0 to 5,000 r/min. For Test 7, the pump speed was manually adjusted to illustrate the pump-valve combination concept. The desired engine temperature was selected as $T_{ed} = 80\,^{\circ}$C for safety considerations.

In all tests, four metrics have been chosen to evaluate the overall performance with the test results summarized in Table III.

TABLE I
Summary of Experiments With Desired Temperature $T_{\rm ed} = 80\,^{\circ}$C (NAMIMO: Nonlinear Adaptive Multiple Input and Multiple Output, NAB: Nonlinear Adaptive Backstepping, SF: State Flow)

Test No.	Controller design	Heat input rate, $q_{\rm in}$ *(kW); Coolant Mass Flow Rate*, $\dot{m}_c$ (kg/s)				Ram Air	
		Time (min)					
		[0, 1)	[1, 11)	[11, 21)	[21, 31]	[0, 1)	[1,31]
1	NAMIMO	20; 1	55; 1	90; 1	20; 1	OFF	OFF
2							ON
3	NAB						OFF
4							ON
5	SF						OFF
6							ON
7	NAMIMO	20; 0.6	55; 0.8	90; 1	20; 0.6		OFF

TABLE II
List of System Model and Controller Parameters

Symbol	Value	Units	Symbol	Value	Units	Symbol	Value	Units
C_e	17.14	kJ/°C	K_1	0.5	-	$\hat{q}_{\rm inl}$	35	kW
Cp_a	1	kJ/kg•°C	K_2	0.5	-	T_{ed}	80	°C
Cp_c	4.18	kJ/kg•°C	$\dot{m}_{c\max}$	1	Kg/s	T_H	82	°C
C_r	8.36	kJ/°C	$N_{f\max}$	5000	r/min	T_L	78	°C
$H_{\max}$	0.95	-	$N_{f\min}$	0	r/min	T_M	80	°C
$H_{\rm nom}$	0.50	-	$N_{f\,\rm nom}$	2500	r/min	$T_{\rm rdh}$	65	°C
$H_{\min}$	0.05	-	$q_{\rm inu}$	100	kW	$T_{\rm rdl}$	55	°C
k_1	0.5	-	$q_{\rm ramu}$	60	kW	$T_{\rm rdm}$	60	°C
k_2	0.5	-	$\hat{q}_{\rm inh}$	75	kW			

1) *Settling time t_{ss}:* Time required for the engine temperature to reach the 2% ($\pm 1.6\,^{\circ}$C) error band after a step heat input change.

TABLE III
TEST RESULTS TO ESTABLISH OVERALL CONTROLLER PERFORMANCE (NAMIMO: NONLINEAR ADAPTIVE MULTIPLE INPUT AND MULTIPLE OUTPUT, NAB: NONLINEAR ADAPTIVE BACKSTEPPING, AND SF: STATE FLOW)

Test No.	Controller Design	Settling Time (s)			Average Radiator Fan Power Consumption, P_f (kW)			Average Pump Power Consumption, P_p (kW)			Mean Absolute Temperature Error (°C)		
		Time Range (min)											
		[1, 11)	[11, 21)	[21, 31]	[1, 11)	[11, 21)	[21, 31]	[1, 11)	[11, 21)	[21, 31]	[1, 11)	[11, 21)	[21, 31]
1	NAMIMO	106.4	129.1	148.0	0.72	3.08	0.31		0.07		0.79	0.85	1.14
2		112.5	137.4	163.1	0.65	3.01	0.22				0.66	0.78	1.60
3	NAB	162.1	336.1	>600	0.53	2.52	0.32				0.83	1.15	2.11
4		190.1	339.0	>600	0.49	2.51	0.12				0.75	1.30	3.40
5	SF	-	-	-	1.26	3.33	0.42				1.12	1.00	1.12
6		-	-	-	1.23	3.32	0.27				1.20	0.99	1.38
7	NAMIMO	110.1	105.1	148.0	0.71	3.10	0.30	0.06	0.07	0.05	0.82	0.79	1.15

2) *Average radiator electric power consumption P_f:* Average total radiator fan power consumption during the test time.
3) *Average pump electric power consumption P_p:* Average pump power consumption during the test time.
4) *Mean absolute error e_M:* Average difference between the measured engine temperature T_e and the desired engine temperature T_{ed} during the tests.

A. NAMIMO Controller

In the laboratory tests, an engine undergoes two moderate thermal loadings which are subsequently removed to evaluate the general cooling system's temperature tracking performance. The results of Test 1 are shown in Fig. 5. The engine and radiator temperature responses in Fig. 5(a) favorably compare with the desired engine and radiator temperature trajectories. Fig. 5(b) displays the engine tracking error versus time which shows that the NAMIMO controller successfully regulated the engine temperature about 80 °C when subjected to three different heat loads with less than a 2 min (120 s) recovery time. The radiator tracking error performance, given in Fig. 5(c), indicates that the controller can adjust the radiator temperature to a desired value. Fig. 5(d) and (e) present the cooling actuator (e.g., valve, radiator fans) operations. As expected, when the heat load increased at times $t = 1\,\text{min}$ and $t = 11\,\text{min}$, the valve opened more each time to allow a greater coolant flow through the radiator. In the meantime, the radiator fan speed was increased to promote external convective heat transfer. The opposite is true when the heat load was removed at time $t = 21\,\text{min}$.

As show in Fig. 5(a), the desired radiator temperature T_{rd} (green dash line) changed automatically subject to the various heat loads. Fig. 6(a) displays the estimated heat input $\hat{q}_{\text{in}}$ versus time for Test 1 which favorably compares with the actual heat input, q_{in}, given in Table I. Note that this value was real time calculated from (22) and integrated over the machine's sampling time scale. Fig. 6(b) displays the corresponding desired radiator temperature, T_{rd}. The selection of the desired radiator temperature per (36) results in the stepped profile. For example, when the heat load was suddenly increased from 55 to 90 kW at time $t = 11\,\text{min}$, the estimated heat load $\hat{q}_{\text{in}}$ climbed from $\hat{q}_{\text{in}} \approx 55\,\text{kW}$ to $\hat{q}_{\text{in}} \approx 90\,\text{kW}$ which exceeded the upper threshold, $\hat{q}_{inh} = 75\,\text{kW}$ at time $t = 12.3\,\text{min}$. To cool the engine, the desired radiator temperature shifted from 60 to 55 °C which produced a sharp increase in the radiator fan speed (4000–5000 r/min as shown in Fig. 5(e)). In contrast, when the heat load was suddenly removed at time $t = 21\,\text{min}$, the estimated heat load decreased to $\hat{q}_{\text{in}} \approx 20\,\text{kW}$. This corresponded to a value below the lower threshold, $\hat{q}_{inl} = 35\text{k}$. Consequently, the desired radiator temperature increased from 55 to 60 °C, and then 65 °C as the thermal load was removed.

The estimated ram air effect, as well as all six fan speeds (defined as global fan speeds), for Tests 1 and 2 is presented in Fig. 7. An interesting observation can be made from these graphs and the average radiator fan power consumption listed in Table III. When the heat load was high ($q_{\text{in}} = 90\,\text{kW}$) at time $t \in [11, 21)\ \text{min}$, the ram air effect was not significant in this study. The difference between the average radiator fan power consumption of Tests 1 (3.08 kW) and 2 (3.01 kW) was only 2.3%. On the other hand, when the heat load was small ($q_{\text{in}} = 20\,\text{kW}$) at time $t \in [21, 31]\ \text{min}$, a greater difference in the radiator fans speed can be noticed. The ram air effect removed most of the heat under this scenario and reduced the radiator power consumption up to 40.9%. The similar phenomenon can be observed in Tests 3–6 per Table III. This phenomenon may be attributed to the experimental test configuration; the axial fan was located in front of CAN bus controlled radiator fan array and heat exchangers. As a result, the air mass flow rate across the radiator generated by the axial fan may be small when compared to the radiator fans if they are operated on high speed. In the vehicle, the ram air effect given in (8) may be greater when the chassis and/or wind speeds are high. As discussed in Case 2, Section B, this phenomenon corresponds to highway operation and a pump–valve combination control strategy may be implemented with the radiator fans shut off.

B. Comparison of Controllers for Overall Performance

The system performance of Tests 1, 3, and 5 are summarized in Fig. 8 to compare the three proposed control strategies. Fig. 8(a) displays the engine tracking error, e, versus time which indicates that the NAMIMO controller offered a much

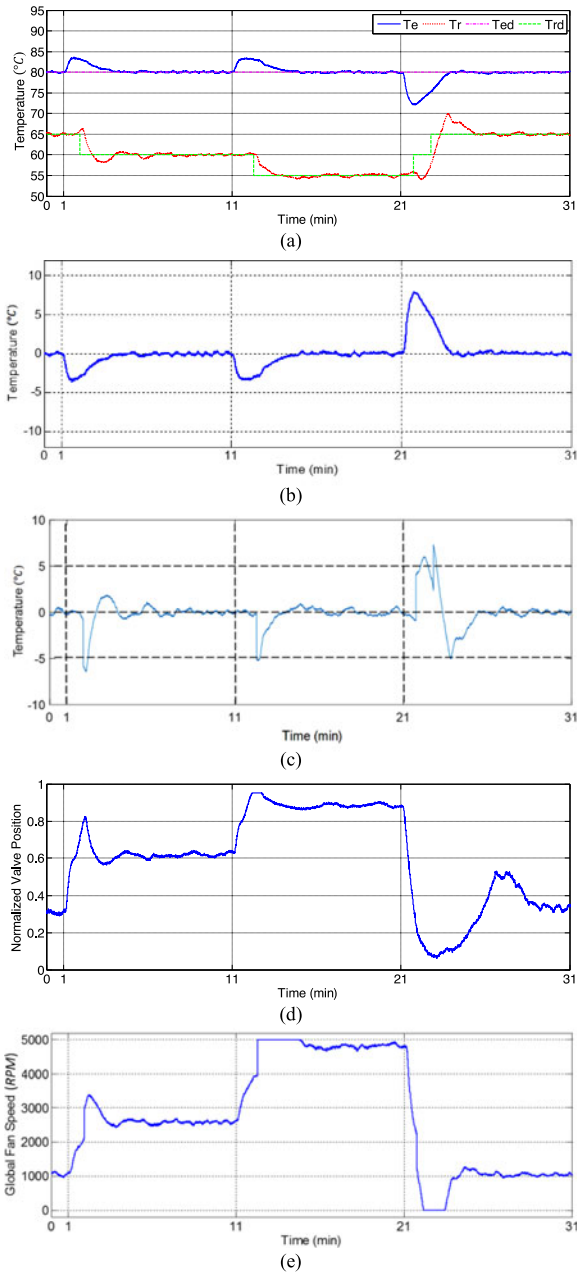

Fig. 5. System response of Test 1. (a) Engine, radiator, and desired radiator temperature, (b) engine temperature tracking error, (c) radiator temperature tracking error, (d) valve position, and (e) global fan speed versus time.

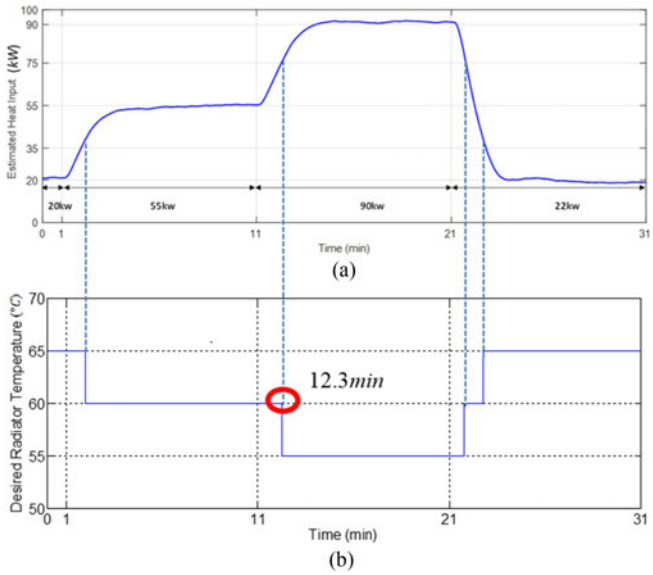

Fig. 6. (a) Estimated heat input, $\hat{q}_{\rm in}$, and (b) desired radiator temperature, T_{rd}, for Test 1 versus time.

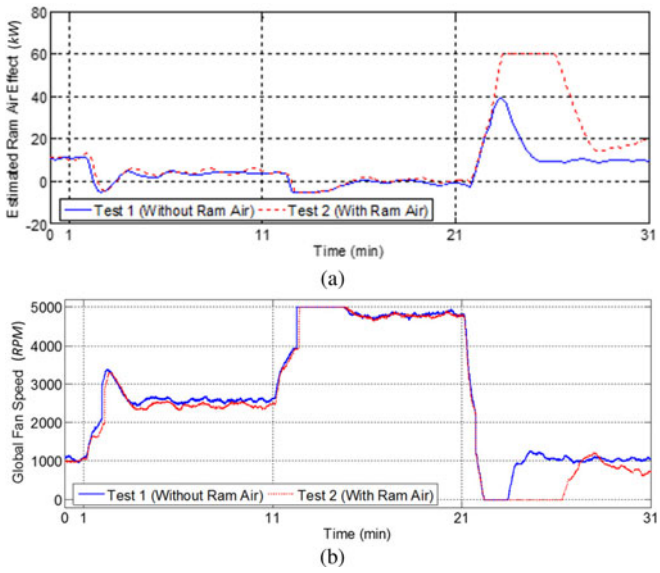

Fig. 7. Compared results for Tests 1 and 2. (a) Estimated ram air effect $\hat{q}_{\rm ram}$ and (b) global fan speed $N_{\rm fan}$ versus time.

faster response than the NAB control law (e.g., 34% faster when comparing Tests 1 and 3 for $t \in [11, 21)$ min according to Table III). The reason for this phenomenon can be attributed to: NAMIMO controller operated the valve position which changed the proportion of the cold and hot coolant that flowed into the engine. On the other hand, the NAB controller adjusted the radiator fans speed which only changed the heat transfer among the different interfaces (e.g., air, metal, and coolant). Further, due to the fixed maximum valve position and pump speed, $u_1 = u_{1\max} = \dot{m}_{c\max} H_{\max}$, the cold coolant kept flowing to the engine node even though the heat load was removed. As a result, the NAB control law showed the worst performance (slowest response) at low heat load conditions $t \in [21, 31]$ min. This phenomenon indicates that the valve-pump setup is indispensable to a cooling system to prevent the engine from being over cooled. Lastly, the SF controller successfully regulated the engine temperature in an $|e| < 5\,^{\circ}$C range.

From a power consumption perspective, Fig. 8(c) and Table III indicate that the NAB control consumes the least radiator fan power followed by the NAMIMO and SF controllers.

C. Pump-Valve Combination

An independent test, Test 7, was performed to study the combination of the system input '1,' $u_1 = \dot{m}_c H$. In this instance, the heat load $q_{\rm in}$ and the ram air effect $q_{\rm ram}$ corresponded to

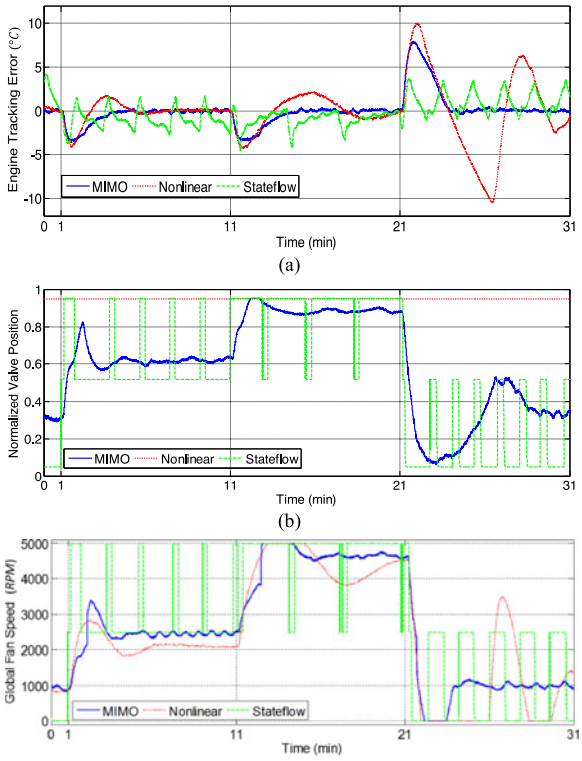

Fig. 8. Compared result for Tests 1, 3, and 5. (a) Engine temperature tracking error, (b) valve position, and (c) global fan speed versus time.

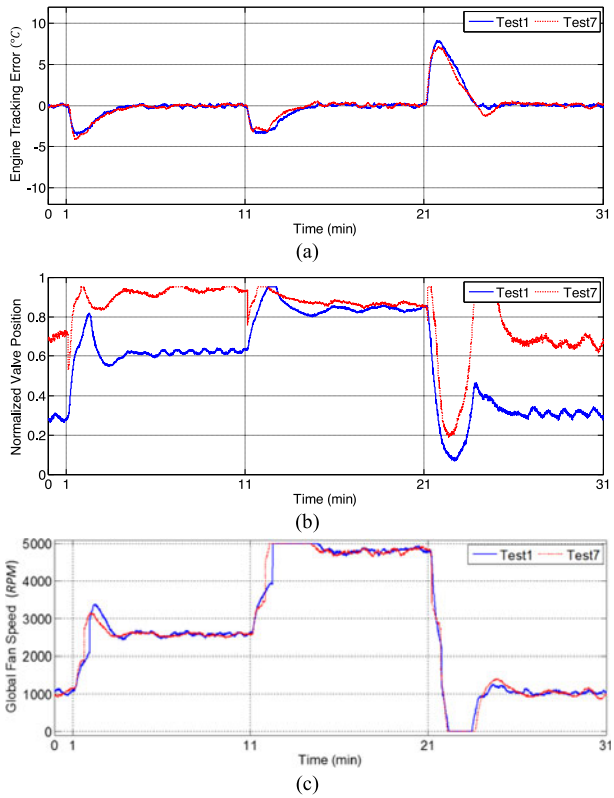

Fig. 9. Compared result for Tests 1 and 7. (a) Engine temperature tracking error, (b) valve position, and (c) global fan speed versus time.

the setting of Test 1. However, the pump speed was manually adjusted over several time ranges. The results in Fig. 9 may be compared with Test 1. From Fig. 9(a) and (c), the coolant flow rate $\dot{m}_c$ does not impact the error tracking performance e, nor the radiator fan operation u_2. The two system inputs u_1 and u_2 were prescribed independently of each other per (20) and (21). Fig. 9(b) illustrates that the coolant flow rate had a significant impact on the valve position. The valve positions coincide when the coolant flow rates were the same, $\dot{m}_c = \dot{m}_{c\max} = 1\,\text{kg/s}$, for Tests 1 and 7 at time $t \in [11, 21)$ min. During another time range, $t \in [1, 11)$ min, the valve opened more in Test 7 than in Test 1 to obtain the same value of system input '1' $u_1 = \dot{m}_c H$. From a power consumption view, when the coolant flow rate decreased in Test 7, the power consumption of the pump decreased as expected (e.g., a 28.6% power saving at time $t \in [21, 31]$ min). This observation indicates that optimized operation may minimize the actuator's power consumption which is an interesting point for future research.

VI. Conclusion

Advanced automotive cooling systems can regulate the internal combustion engine temperature within a specified temperature range while minimizing subsystem power consumption. In this paper, the cooling system dynamics and control laws were derived and applied to an experimental testing bench features with a 6.8 L engine. The proposed NAMIMO control law operated the valve position and radiator fan speed. For comparison purposes, a NAB control strategy and a SF control law were introduced. The test results showed that the NAMIMO controller can successfully regulate the engine temperature to the desired value and compensate for unknown heat loads and ram air effects. Although the NAB controller consumed the least electric actuator power, the performance was characterized by a slow response and weakness at low heat input conditions. The SF controller, although it demonstrated greater temperature oscillation and consumed much more actuator power, was easy to realize and maintained the coolant temperature in an acceptable range. The test results also revealed that as the ram air effect decreased, the commanded radiator fan speed increased as expected. Finally, an independent test demonstrated that the operation of the pump-valve combination has the potential to further minimize the actuator power. This research offers insight into the future work regarding on-engine/in-vehicle testing.

Appendix A
Design of Nonlinear Adaptive Backstepping Controller

In an earlier radiator fan control study [11], a Lyapunov based nonlinear backstepping adaptive controller was developed. The controller design realizes minimum radiator fan power consumption for different operating conditions. As a result, the pump and valve operations are scheduled at the maximum combination, $u_1 = u_{1\max}$. The ram air effect was not considered

when the controller was developed so equation (8) becomes

$$\begin{bmatrix}\dot{T}_e\\ \dot{T}_r\end{bmatrix} = \begin{bmatrix}\dfrac{-u_{1\max}Cp_c}{C_e} & \dfrac{u_{1\max}Cp_c}{C_e}\\ \dfrac{u_{1\max}Cp_c}{C_r} & \dfrac{-u_{1\max}Cp_c - u_2Cp_a}{C_r}\end{bmatrix}\begin{bmatrix}T_e\\ T_r\end{bmatrix} + \begin{bmatrix}\dfrac{q_{\text{in}}}{C_e}\\ \dfrac{u_2Cp_fT_\infty}{C_r}\end{bmatrix} \tag{A.1}$$

From equation (A.1), the control problem becomes an adaptive integrator backstepping problem with an unknown parameter, q_{in}. The system input, $u_2 = \dot{m}_f$, directly impacts the radiator temperature, T_r. The radiator temperature affects the engine temperature, T_e, via the coolant flow heat transfer. The controller may be designed as

$$u_1 = u_{1\max} = \dot{m}_{c\max}H_{\max}$$

$$u_2 = \left[\phi_1 + \phi_2 + \phi_3 + \phi_4 + K_2\left(T_{RD} - T_r\right) + \frac{u_{1\max}Cp_c}{C_e}e\right] \tag{A.2}$$

where

$$\phi_1 = \frac{-\dot{\hat{q}}_{in1}}{u_{1\max}Cp_c} \tag{A.3}$$

$$\phi_2 = \frac{C_eK_1 - u_{1\max}Cp_c}{u_{1\max}Cp_c}\left[\frac{u_{1\max}Cp_c(T_{ed} - e - T_r)}{C_e}\right] \tag{A.4}$$

$$\phi_3 = -\frac{u_{1\max}Cp_c(T_e - T_r)}{C_r} \tag{A.5}$$

$$\phi_4 = -\frac{C_eK_1 - u_{1\max}Cp_c}{u_{1\max}Cp_c}\hat{q}_{in2} \tag{A.6}$$

$$T_{RD} = \frac{u_{1\max}Cp_cT_{ed} + (C_eK_1 - u_{1\max}Cp_c)\,e - \hat{q}_{in1}}{u_{1\max}Cp_c} \tag{A.7}$$

$$\hat{q}_{in1} = -\frac{1}{C_e}\int_{t_0}^{t} e d\tau \tag{A.8}$$

$$\hat{q}_{in2} = -\frac{C_eK_1 - u_{1\max}Cp_c}{u_{1\max}Cp_cC_e}\int_{t_0}^{t}\left(T_{RD} - T_r\right)d\tau \tag{A.9}$$

The variable T_{RD} is an intermediate system input, while the terms K_1 and K_2 denote the controller gains.

When applying this controller to the system, the radiator fans will be operated to regulate the engine temperature at the desired value, T_{ed}, and accommodate the various heat loads, q_{in}. Interested readers are referred to reference [11] for a complete derivation of the control law including stability analysis, and experimental validation.

APPENDIX B
STATE FLOW CONTROLLER DESIGN

If the system is constrained by the available engine control unit's (ECU) speed/memory, a logic based control law may be introduced to adjust the valve's position and radiator fan speed. State flow (SF) control, used to control automotive subsystems, considers the logical expressions of state machines. A SF controller switches between different outputs according to the system states and pre-programmed control law.

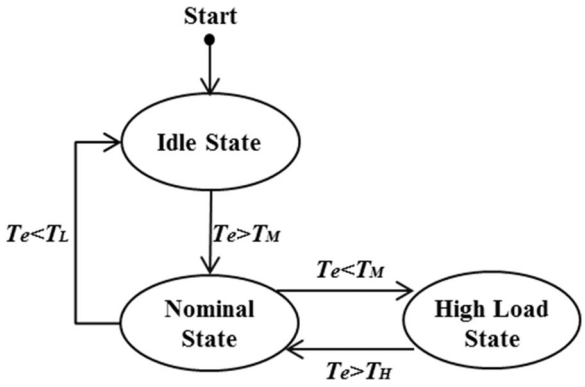

Fig. 10. State flow control structure.

In this study, the control states are defined as *Idle, Nominal, High load* The logic flow diagram is shown in Fig. 10. The variables T_H, T_L, and T_M are the selected thresholds that have been chosen according to baseline calibrations and listed in Table II. The operations of the actuators in each state will be briefly described.

Idle State: When the engine temperature, T_e, is below the lower threshold, T_L, which denotes a warm up/cold start condition, the system inputs 1 and 2 are operated at their lower limits to keep the engine temperature increasing toward the desired working range. In mathematical form, $[u_1, u_2] = [u_{1\min},\ u_{2\min}]$. Once the engine temperature reaches the middle threshold, T_M, the system will shift to the nominal state.

Nominal State: In the nominal state, the valve-pump combination, and the radiator fans are operated at their normal condition, $[u_1, u_2] = [u_{1\text{nom}},\ u_{2\text{nom}}]$. Considering the thermal inertia, this system condition may be switched to from either the idle state when the engine is too hot, $T_e > T_M$, or from the high load state when the engine is too hot, $T_e < T_M$.

High Load State: If the engine temperature exceeds the prescribed higher threshold, T_H, then the controller transitions to the high load state. The system inputs are all operated at their maximum capacity to reject heat from the engine. The cooling control behavior will be realized as $[u_1, u_2] = [u_{1\max},\ u_{2\max}]$.

As mentioned in Section V, the coolant mass flow rate is a constant, $\dot{m}_c = \dot{m}_{c\max}$. The state of system input '1' was represented by the valve position, $u_{1\min,\text{nom},\max}$, as reflected by $H_{\min,\text{nom},\max}$. The system input '2' state, $u_{2\min,\text{nom},\max}$, corresponding to the air mass flow rate, is reflected by the radiator fan motor speed, $N_{f\min,\text{nom},\max}$. The parameter values for $H_{\min,\text{nom},\max}$ and $N_{f\min,\text{nom},\max}$ can be found in Table II.

REFERENCES

[1] Environmental Protection Agency and Dept. Transp., Nat. Highway Traffic Safety Admin., "2017 and later model year light-duty vehicle greenhouse gas emissions and corporate average fuel economy standards; final rule," *Fed. Register*, vol. 77, no. 199, pp. 62623–63200, 2012.

[2] *Fact Sheet—EU28 Light-Duty Vehicle Efficiency Standards*, Int. Council Clean Transp., Washington, DC, USA, 2014.

[3] *Light-Duty Automotive Technology, Carbon Dioxide Emissions, and Fuel Economy Trends: 1975 Through 2014*, Environmental Protection Agency, Washington, DC, USA, 2014.
[4] J. Heywood, *Internal Combustion Engine Fundamentals*. New York, NY, USA: McGraw-Hill, 1988.
[5] R. Page, W. Hnatczuk, and J. Kozierowski, "Thermal management for the 21st century—Improved thermal control & fuel economy in an army medium tactical vehicle," in *Proc. SAE Veh. Therm. Manage. Syst. Conf. Exhib.*, Toronto, ON, Canada, May 2005, Paper 2005-01-2068.
[6] S. Sermeno, E. Bideaux, T. Morgan, and D. Nguyen, "Heavy duty vehicle cooling system auxiliary load management control: Evaluating the maximum gain of implementing an advanced control strategy," in *Proc. SAE Commercial Veh. Eng. Congr*, Rosemont, IL, USA, Oct. 2014, Paper 2014-01-2341.
[7] J. Wagner, I. Paradis, E. Marotta, and D. Dawson, "Enhanced automotive engine cooling system—A mechatronics approach," *Int. J. Veh. Des.*, vol. 28, nos. 1–3, pp. 214–240, 2002.
[8] H. Kim, J. Shon, and K. Lee, "A study of fuel economy and exhaust emission according to engine coolant and oil temperature," *J. Therm. Sci. Technol.*, vol. 8, no. 1, pp. 255–268, 2013.
[9] P. Setlur, J. Wagner, D. Dawson, and E. Marotta, "An advanced engine thermal management system: Nonlinear control and test," *IEEE/ASME Trans. Mechatronics*, vol. 10, no. 2, pp. 210–220, Apr. 2005.
[10] T. Wang, A. Jagarwal, J. Wagner, and G. Fadel, "Optimization of an automotive radiator fan array operation to reduce power consumption," *IEEE/ASME Trans. Mechatronics*, vol. 20, no. 5, pp. 2359–2369, Oct. 2015.
[11] T. Wang and J. Wagner, "Advanced automotive thermal management—Nonlinear radiator fan matrix control," *Control Eng. Pract.*, vol. 41, pp. 113–123, 2015.
[12] M. Salah, P. Frick, J. Wagner, and D. Dawson, "Hydraulic actuated automotive cooling systems—Nonlinear control and test," *Control Eng. Pract.*, vol. 17, pp. 609–621, May 2009.
[13] M. Salah, T. Mitchell, J. Wagner, and D. Dawson, "A smart multiple loop automotive cooling system model, control, and experimental study," *IEEE/ASME Trans. Mechatronics*, vol. 15, no. 1, pp. 117–124, Feb. 2010.
[14] X. Tao and J. Wagner, "A thermal management system for the battery pack of a hybrid electric vehicle: Modeling and control," *Proc. Inst. Mech. Eng., Part D: J. Automob. Eng.*, vol. 230, no. 2, pp. 190–201, 2016.
[15] S. Butt, R. Prabel, and H. Aschemann, "Robust input—Output linearization with input constraints for an engine cooling system," in *Proc. Amer. Control Conf.*, Portland, OR, USA, Jun. 2014, pp. 4555–4560.
[16] S. Butt, R. Prabel, R. Grimmecke, and H. Aschemann, "Nonlinear model-predictive control for an engine cooling system with smart valve and pump," in *Proc. Int. Conf. Methods Models Autom. Robot.*, Miedzyzdroje, Poland, Sep. 2014, pp. 520–525.
[17] M. Khodabakhshian, L. Feng, and J. Wikander, "Predictive control of the engine cooling system for fuel efficiency improvement," in *Proc. Autom. Sci. Eng. Conf.*, Taipei, Taiwan, Aug. 2014, pp. 61–66.
[18] T. Wang and J. Wagner, "A smart engine cooling system—Experimental study of temperature transient responses," in *Proc. SAE World Congr.*, Detroit, MI, USA, Apr. 2015, Paper 2015-01-1604.
[19] D. Allen and M. Lasecki, "Thermal management evolution and controlled coolant flow," in *Proc. Veh. Therm. Manage. Syst. Conf.*, Nashville, TN, USA, May 2001, Paper 2001-01-1732.

Tianwei (Thomas) Wang received the B.S. and M.S. degrees in mechanical engineering from the East China University of Science and Technology, Shanghai, China, and the Ph.D. degree from the Mechanical Engineering Department, Clemson University, Clemson, SC, USA. During his time at Clemson University, his research interests included system dynamics, nonlinear and intelligent control theory, automotive powertrain thermal management, and 3-D visualization based engineering education. He is a Controls Engineer at Diverse Automation, SC, working on industrial automation, robotics, and control system development.

John Wagner (SM'10) received the B.S., M.S., and Ph.D. degrees in mechanical engineering from the State University of New York at Buffalo and Purdue University. He was previously on the engineering staff at Delco Electronics, designing and testing automotive electronic control systems. During this time period, he held a variety of technical positions, including Supervisor of the Simulation & Hardware-in-the-Loop and the Electronic Spark Control Groups. He serves as the Faculty Advisor for the Clemson University Society of Automotive Engineers (SAE) chapter. His research interests include nonlinear control theory, smart cooling systems, diagnostic/prognostic strategies, and mechatronic system design with application to transportation and power generation systems. His multi-disciplinary research activities emphasize a collaborative teaming approach with both industrial and government sponsors. He has established the multi-disciplinary Mechatronics and Automotive Research Laboratory in the Mechanical Engineering Department and collaborates with the Wind Turbine Testing Facility in Charleston, SC, USA. He teaches dynamic systems and control courses; he developed the Rockwell Automation Mechatronics System Design Educational Laboratory, which features a variety of bench top electromechanical experiments. Dr. Wagner is a Licensed Professional Engineer and a Fellow of the American Society of Mechanical Engineers.